



Spatial Characterization of Black Carbon Mass Concentration in the Atmosphere of a Southeast Asian Megacity: An Air Quality Case Study for Metro Manila, Philippines

Honey Dawn Alas^{1,2*}, Thomas Müller¹, Wolfram Birmili^{1,6}, Simonas Kecorius¹, Maria Obiminda Cambaliza^{2,3}, James Bernard B. Simpas^{2,3}, Mylene Cayetano⁴, Kay Weinhöhl¹, Edgar Vallar⁵, Maria Cecilia Galvez⁵, Alfred Wiedensohler¹

¹ Leibniz Institute for Tropospheric Research, 04318 Leipzig, Germany

² The Manila Observatory, Quezon City 1101, Philippines

³ Department of Physics, Ateneo de Manila University, Quezon City 1108, Philippines

⁴ Institute of Environmental Science and Meteorology, University of the Philippines, Quezon City 1101, Philippines

⁵ Applied Research for Community, Health and Environment Resilience and Sustainability (ARCHERS), De La Salle University, Manila 1004, Philippines

⁶ Federal Environment Agency, 14195 Berlin, Germany

ABSTRACT

Black carbon (BC) particles have gathered worldwide attention due to their impacts on climate and adverse health effects on humans in heavily polluted environments. Such is the case in megacities of developing and emerging countries in Southeast Asia, in which rapid urbanization, vehicles of obsolete technology, outdated air quality legislations, and crumbling infrastructure lead to poor air quality. However, since measurements of BC are generally not mandatory, its spatial and temporal characteristics, especially in developing megacities, are poorly understood. To raise awareness on the urgency of monitoring and mitigating the air quality crises in megacities, we present the results of the first intensive characterization experiment in Metro Manila, Philippines, focusing on the spatial and diurnal variability of equivalent BC (eBC).

The average mass concentration of eBC at the urban background station (UBS) was $7.0 \pm 4.8 \mu\text{g m}^{-3}$ while at roadside (RS), hourly concentrations reached maximum values of $138 \mu\text{g m}^{-3}$, levels that are significantly higher than in European cities. At RS, the diurnal cycles of eBC mass concentration were connected most strongly with traffic dynamics and street configuration, while a notable influence of planetary boundary layer evolution was observed in the UBS. Results of mobile measurements conducted multiple times along two fixed routes showed high spatial variability ranging from 3–80 $\mu\text{g m}^{-3}$ within a 500-m radius. Alarmingly, the highest concentrations were found in the most crowded areas where people spend more than eight hours a day.

Keywords: Black carbon; Megacity; Spatial and diurnal variability; Mobile measurements.

INTRODUCTION

Megacities (cities with more than 10 million people) in less developed regions continue to suffer from high levels of air pollution and its consequences as a result of rapid urbanization and economic growth (WHO, 2016). Criteria pollutants (gaseous and particulate matter or PM) are being monitored and regulated according to WHO guidelines (WHO, 2006) in these megacities. However, black carbon

(BC) particles - nanoparticles that carry toxic materials (Nemmar *et al.*, 2002; WHO, 2012) which are linked to various diseases (Krzyzanowski *et al.*, 2005; WHO, 2007; HEI, 2010) - remain unregulated (Krzyzanowski and Cohen, 2008). Despite growing efforts to monitor BC in fixed locations, it is still extremely challenging to model its spatial distribution and estimate personal exposure levels in a microscale since BC is highly variable in space and time (Peters *et al.*, 2013; Rakowska *et al.*, 2014).

In recent years, atmospheric researchers have started to shift their attention from stationary monitoring towards mobile pollutant measurements. Mobile measurements are able to capture features of the considerable spatial variability of pollutant concentrations typically found in urban atmospheres. On the technical side, mobile measurements

*Corresponding author.

Tel.: +49 341 2717 7060; Fax: +49 341 2717 99 7060

E-mail address: alas@tropos.de

require robust and portable devices that are typically mounted on mobile platforms such as backpacks of pedestrians, bicycles, and vehicles. High time resolution, in the order of seconds or minutes, is required to detect spatial gradients of pollutant concentrations across selected itineraries. This method has been proven useful in different scientific applications such as evaluating representativeness of fixed stations (Nerriere *et al.*, 2005), determining emission factors (Karjalainen *et al.*, 2014; Jezek *et al.*, 2015), and developing land use regression models (Ruths *et al.*, 2014; Ghassoun *et al.*, 2015). More importantly, it can increase the accuracy in estimating personal exposure to pollutants (Adams *et al.*, 2002; Birmili *et al.*, 2013; Peters *et al.*, 2014; Patton *et al.*, 2016; Williams and Knibbs, 2016). Furthermore, the high-resolution data of mobile platforms is effective in validating modelled spatial distribution of pollution (Dons *et al.*, 2014). We note that most mobile measurement campaigns have been conducted in European cities (Schneider *et al.*, 2008; Dons *et al.*, 2011, 2012; Birmili *et al.*, 2013; Dons *et al.*, 2013; Van Poppel *et al.*, 2013; Peters *et al.*, 2014; Van den Bossche *et al.*, 2015, 2016) and North America (Westerdahl *et al.*, 2005; Fruin *et al.*, 2008; Westerdahl *et al.*, 2008; Zhu *et al.*, 2008; Levy *et al.*, 2014; Baldwin *et al.*, 2015).

To date, there is a notable lack of representative data on the spatial distribution of BC in developing and emerging countries (Hung *et al.*, 2014; Rakowska *et al.*, 2014; Kim *et al.*, 2015). The air quality situation in megacities of those countries is often precarious, because pollutant sources and populations intermingle in a dense fashion on limited space. Moreover, there tend to be more complex street configurations, outdated vehicle fleet, intense industrial emissions, less stringent regulations, and consequently, more people at risk.

An example is the megacity of Metro Manila in the Philippines. Metro Manila is home to 12 million people and has a population density of 21 thousand people per square kilometre (Philippine Statistics Authority, 2016). Consequently, it has the highest number of registered motor vehicles compared with other cities in the country, with a reported number of 2.2 million (Philippine Land Transportation Office, 2015). With these statistics, it is not surprising that 90% of emissions in this city is from mobile sources (Environmental Management Bureau, 2012). Due to its unique topography (Manila Bay on its West and the Laguna Lake on the East), the air quality of Metro Manila is mainly urban-originated and the influence of long-range-transported aerosol is minimal (Kim Oanh *et al.*, 2006). In 1999, the Clean Air Act was established to improve air quality. Under this law, the limits were set for criteria pollutants including PM₁₀ (150 and 60 $\mu\text{g m}^{-3}$ for daily and annual mean, respectively) and more recently (January 2016) PM_{2.5} (50 and 25 $\mu\text{g m}^{-3}$ for daily and annual mean, respectively). Long-term observations show that annual PM₁₀ levels from 2000–2008 have never exceeded these national limits (Zhu *et al.*, 2012). However, for PM_{2.5} during the dry season (see Supplementary Material), the average concentrations in mixed and traffic sites are 18.7 $\mu\text{g m}^{-3}$ and 58.4 $\mu\text{g m}^{-3}$, respectively. In the mixed site, 57% of PM_{2.5} is soot (10.7 $\mu\text{g m}^{-3}$) while at a traffic site, soot is 63% of PM_{2.5} (Simpas *et al.*, 2014). Consequently, in 2008,

Hopke *et al.* (2008) reported that in terms of elemental black carbon (the black carbon content of the fine fraction filters was measured using a reflected light instrument), Metro Manila has the second highest concentration in Asia, next to Dhaka, Bangladesh. Clearly, the current criteria does not provide enough information on the air quality situation in Metro Manila, and possibly in other megacities.

To address this, the Metro Manila Aerosol Characterization Experiment (MACE 2015) was initiated. This was the first intensive monitoring of air pollution in Metro Manila, conducted in the summer of 2015. The general objective of the pilot case study was to investigate the diurnal and spatial characteristics of black carbon in the megacity Manila. MACE 2015 also aimed to provide evidence on the need to update and improve existing air quality policies, and to suggest BC as a more suitable criterion for roadside emissions, since it can provide a deeper understanding of the health impacts of air pollution more than PM₁₀ and PM_{2.5}. Specifically, this study focuses on following objectives: 1) to determine the spatial and diurnal variability of equivalent BC (eBC, a proxy for soot; a nomenclature suggested by Petzold *et al.*, 2013 when describing BC measured optically), 2) to determine the factors that drive these variabilities, 3) to estimate the contribution of local traffic emissions to ambient air quality, and 4) to compare the observed eBC mass concentrations in Metro Manila with other cities, and 5) to validate models of spatial distribution of eBC mass concentration.

To achieve these objectives, eBC mass concentrations were measured at three sites, at two roadside sites and at an urban background station. The influence of meteorology, traffic schemes, and street topography were investigated. Mobile measurements were performed along two fixed routes which covered different microenvironments and exposure scenarios. Background correction was also performed to determine the contribution of local traffic sources to urban air quality. Results from this study can raise awareness on the current air quality situations that developing and emerging megacities experience, potentially influence the air quality policies, and help increase the accuracy of environmental and health studies in these regions.

EXPERIMENT DESIGN

The measurements were performed in the highly urbanized megacity of Metro Manila, the country's National Capital Region (NCR) that is an agglomerate of 17 local government units. The climate of the region can be divided into two seasons: the wet season, which starts from May to October, and the dry season, which is from November to April. We decided to measure during the dry season since the data that can be gathered during the wet season, when there are torrential rains and typhoons, may be less relevant due to wash out.

Mean values for temperature, relative humidity, and pressure during the field campaign have been $29.9 \pm 2.8^\circ\text{C}$, $66.0 \pm 12.2\%$, and 1012.2 ± 2.6 hPa, respectively. The temperature was highest during the afternoon ($\sim 33^\circ\text{C}$). The meteorological conditions did not vary significantly throughout

the campaign except that more rain events were recorded beginning in May (six rain events were recorded in April to middle of May while only four during middle of May to mid-June). These rain events in May together with the shift of prevailing wind direction from east to southwest (not shown here) signal the onset of the Southwest monsoon season for the country as winds coming from the moist Southwest region blow through the Philippines (Chen and Chen, 1995). Wind data from the automated weather station (AWS) and sonic anemometer showed high variability of winds all throughout the day but, on average, stronger winds were experienced during the afternoon ($1.9 \pm 0.7 \text{ m s}^{-1}$) than in the morning ($0.5 \pm 0.5 \text{ m s}^{-1}$).

Due to the high number of motor vehicles, the local government units implement varying traffic schemes in major thoroughfares, such as the *Truck Ban* and *Number Coding* schemes to ease the heavy traffic at identified periods. The goal of the *Truck Ban scheme* is to ease traffic congestion by not allowing trucks on the roads during rush hours (6:00 AM to 9:00 AM and 5:00 PM to 9:00 PM). In between these times is the *Truck Ban window*, the time of day when trucks are allowed on major thoroughfares. The *Number Coding* scheme restricts private cars with plate numbers that end with a specific number from using major thoroughfares during rush hour on a given day. For example,

private vehicles with plate number ending in 1 and 2 are not allowed on the major thoroughfares between 7:00 AM to 10:00 AM and 3:00 PM to 7:00 PM on Mondays (Metro Manila Development Authority, <http://www.mmda.gov.ph/>). These schemes, however, are not uniform for all the roads in Metro Manila, as mentioned, and are applicable only to major thoroughfares. For example, the *Truck Ban* scheme is absolute along a part of Taft Avenue that is within the territory of Manila, while in other neighbouring cities, trucks are prohibited only at certain periods.

Therefore, the experiment was designed to also investigate how these traffic schemes affect the air quality by measuring at roadside sites with varying traffic schemes. Fig. 1 shows the location of the study areas and observation sites and Table 1 lists the site descriptions and measurement periods.

Fixed Station – Urban Background Station (UBS)

The fixed station was situated in the fourth floor of a building (~70 masl) of a research institution, The Manila Observatory (MO; 14,636°N, 121,078°E) (Fig. 2(c)), which is located within the 210-acre campus (~57 masl) of the Ateneo de Manila University (ADMU). Located 250 m west of this site is Katipunan Avenue, which is a 6 to 8-lane avenue frequented by trucks, private cars, and public utility vehicles (PUVs). South of this location, ~350 m

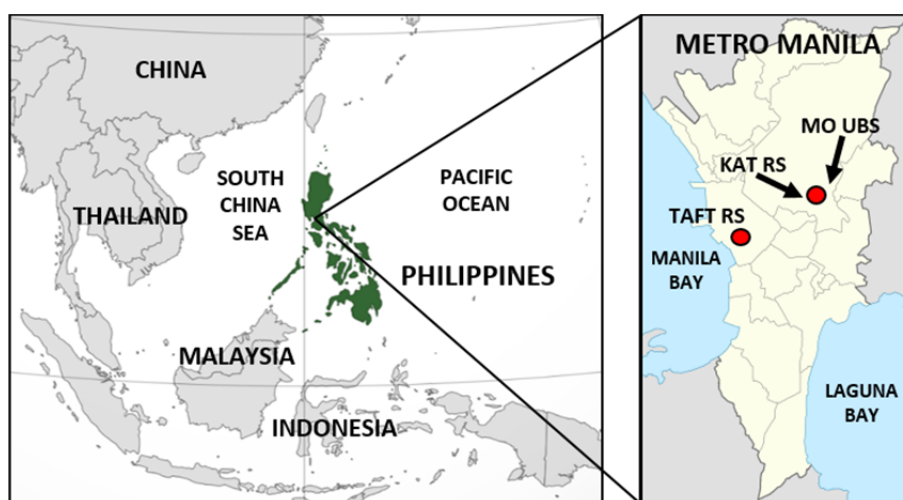


Fig. 1. Map of Metro Manila indicating the approximate location of the measurement sites. Taft Roadside – *TAFT RS* is 12 km away from MO urban background station – *MO UBS* and Katipunan Roadside – *KAT RS* while the latter sites are ~380 m apart. Bodies of water that surround the country and the metropolitan are indicated in the figure. Source: www.d-maps.com.

Table 1. Description of selected observation sites.

Site	Type	Traffic condition (PCU/hr ^a)	Site name	Duration (dd/mm)
MO Building	Urban background (UBS)	-	MO UBS	01/04–10/06
Katipunan Avenue	Roadside (RS)	288 000 ^b	KAT RS	01/04–05/05
MO ground level	Urban background	-	MO GL	Inter-comparison 07/05–14/05
Taft Avenue	Roadside (RS)	80 000 ^c	TAFT RS	17/05–10/06

^a passenger car unit/hour. 2012 traffic data; source: JICA 2014.

^b Traffic information of Circumferential Road 5 (C-5 = 26.8 km) where Katipunan Avenue is a part of.

^c Traffic information of Radial Road 2 (R-2 = 6.7 km) which is Taft Avenue.

away, is the intersection between four main thoroughfares: Marcos Highway, Bonifacio Avenue, Aurora Boulevard and Katipunan Avenue. There is a terminal for a special kind of PUV in this intersection called the *jeepneys* (see Fig. S1). These are the cheapest and most popular means of transportation in the country that run on outdated engines powered by diesel fuel.

This MO site, referred to as “MO UBS” for the rest of the paper, was therefore chosen to investigate the properties of the urban background aerosol.

Sites for Roadside Measurements

The aerosol container was first placed ~2 m away from the roadside of Katipunan Avenue and referred to as “KAT RS” (14.635°N, 121.075°E) (Fig. 2(a)). This avenue is a major thoroughfare that runs north to south. On the west side of this road are different establishments with few high-rise buildings. On its east are two campuses with open green spaces. This road experiences heavy traffic during rush hour (9050 passenger cars/hour, Ateneo Traffic Group 2012 Report) and Truck Ban window hours.

After five weeks at KAT RS, the aerosol container was brought close to MO UBS, but at ground level, referred to as “MO GL”, for a week (Fig. 2(d)). North of the aerosol container was MO’s main building (where MO UBS is located) and another building on its south. On its west and east side are open spaces. Northwest of MO GL was an opening to a main road within the ADMU Campus. This period of the field campaign served as the inter-comparison week for the instruments in the aerosol container, MO UBS station, and aerosol backpack.

For the last four weeks of the campaign, the aerosol container was transported to the second roadside site, referred to as “TAFT RS” (Fig. 2(b)) located on Taft Avenue (~12 masl; 14.566°N, 120.994°E) and adjacent to the De La

Salle University (DLSU), which is 12 km southwest of MO UBS (Fig. 1). Taft Avenue is a 4 to 6-lane major thoroughfare that crosses three Metro Manila cities. TAFT RS is 1 km away from the coast of the Manila Bay. Surrounding the site are built-up areas of residential and commercial establishments and a railway track is on the center island traversing the avenue. This avenue is an arterial road that experiences 80,000 passenger car unit - hours of traffic volume (JICA, 2014).

Mobile Measurements

The mobile measurements (hereto, termed as “runs”) were designed to capture the distribution of eBC mass concentration around MO UBS and the aerosol container, using portable devices. Runs were carried out by two “runners” composed of a “carrier” and a “companion”. The runners walked with normal walking paces and took notes of important information such as traffic congestions, construction sites, and detours. Each run lasts approximately one hour.

The runners followed a pre-determined route per roadside site, strategically designed to investigate eBC mass concentrations of different microenvironments. The first route (Fig. 3(a)), referred to as Katipunan Route, is 5.5 km long and included the ADMU campus, MO UBS, Katipunan Avenue, KAT RS, and a residential area on the west side of Katipunan Avenue. The second route (Fig. 3(b)) referred to as Taft Route, was performed when the aerosol container was at TAFT RS. The route is 5 km long and included the closed area of DLSU campus, along Taft Avenue, and dense residential and commercial areas east of Taft Avenue.

Runs were performed twice a day. For the Katipunan route, the first run was at 2:00 PM to capture the Truck Ban window hours and the second run at 5:00 PM during evening rush hour. For the Taft route, the first run was at

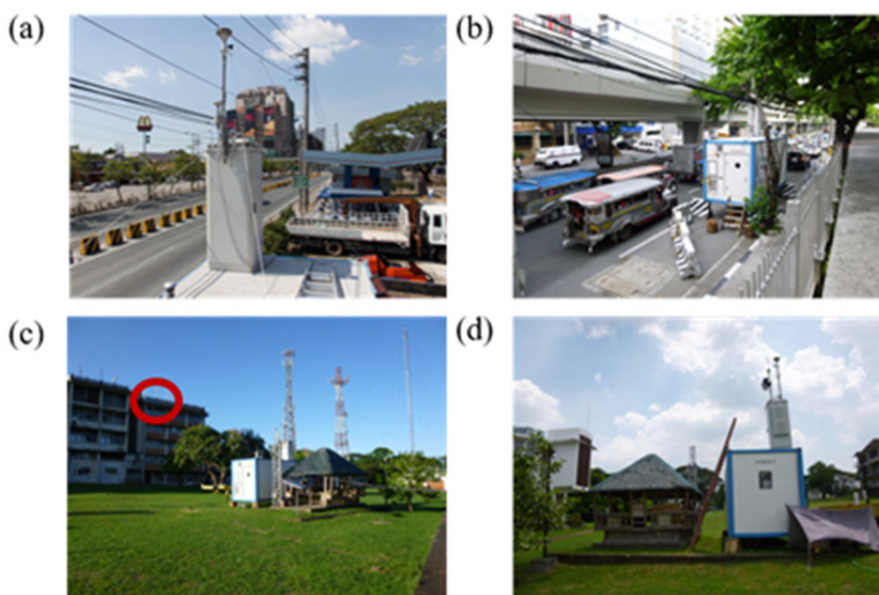


Fig. 2. Illustrations of the measurement sites: (a) KAT RS, (b) TAFT RS, (c) MO UBS – with aerosol inlet and laboratory encircled in red, and (d) the aerosol container at ground level – MO GL – during the inter-comparison week in the urban background region. Description of the sites are listed in Table 1.

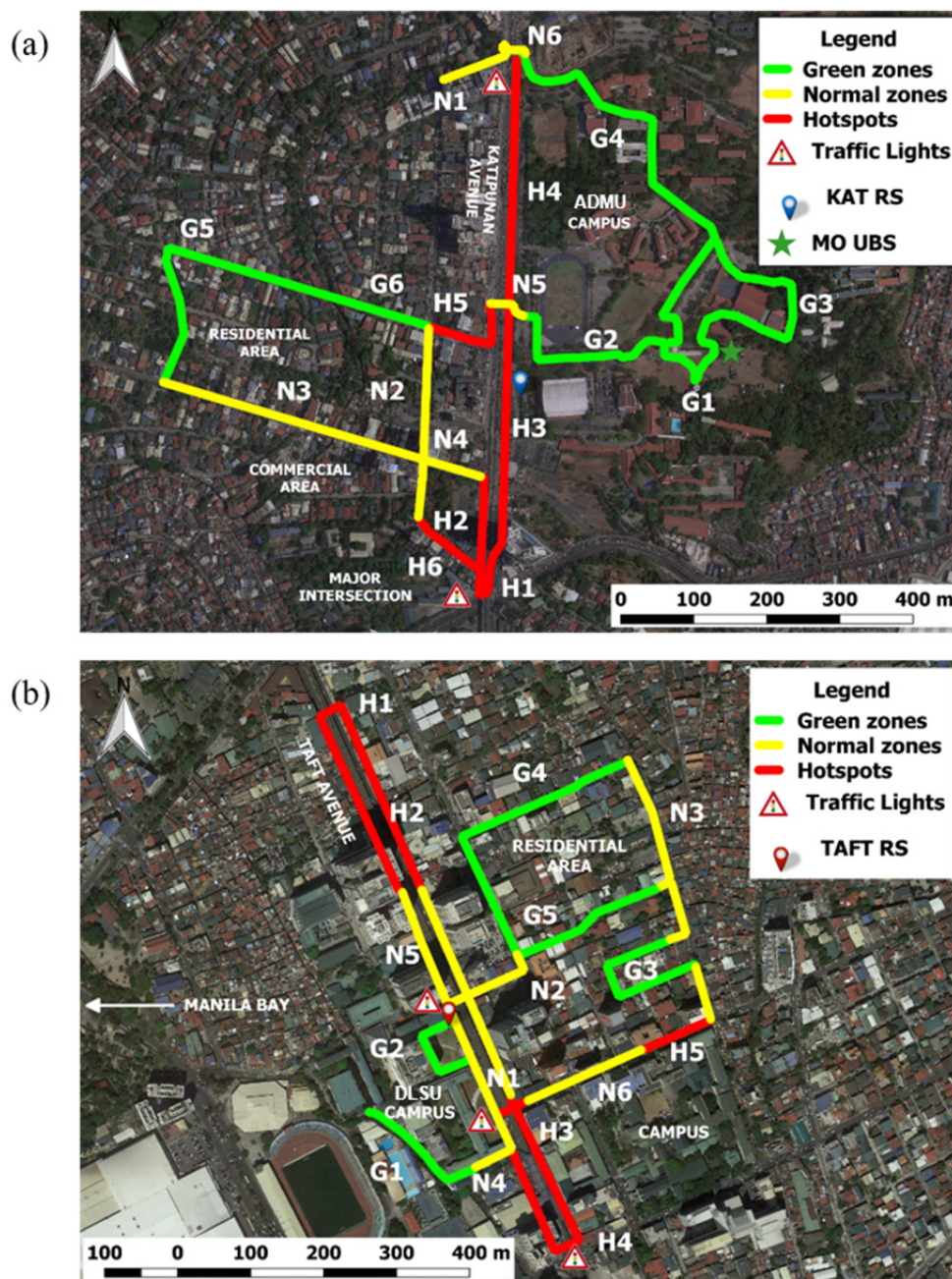


Fig. 3. Classification of the (a) Katipunan route and (b) Taft route according to green zones (green), normal zones (yellow), and hotspots (red). Each zone is labelled: G1–G6 for the green zones, N1–N6 for the normal zones, and H1–H6 for the hotspots. White arrow points to the North. *Source: Visualized through QGIS using Google Earth.*

1:00 PM, during office hours (there was no Truck Ban window along the Manila territory of Taft Avenue), and the second run at 5:00 PM, during the evening rush hour.

INSTRUMENTATION

Measurement Setup

MO UBS

The aerosol was sampled through a stainless steel inlet that began from the rooftop of the MO building, then entered a temperature (23–25°C) controlled room through a window. The inlet system had a PM₁₀ inlet (Rupprecht & Patashnick

Co., Inc. Thermo), which allowed the measurement of particles smaller than an aerodynamic diameter of 10 μm at a flow rate of 16.7 L min⁻¹. The PM₁₀ inlet was connected to a 1.5 m Nafion®Permapure dryer (Wiedensohler *et al.*, 2013). Since outdoor temperatures are in the range of 30–35°C, the low temperature in the room caused high humidity in the sampled air. The dryer kept the relative humidity of the sampled air below 30%. Inside the MO UBS room, the aerosol was introduced into an isokinetic flow splitter, which then fed the aerosol into the different instruments through stainless steel/conductive tubing (Wiedensohler *et al.*, 2013). Installed at MO UBS were an

absorption photometer (Multi-Angle Absorption Photometer or MAAP Model 2012, Thermo, Inc., Waltham, MA USA) and mobility and aerodynamic particle size spectrometers (Mobility Particle Size Spectrometer or MPSS; TROPOS, Germany, Wiedensohler *et al.*, 2012; Aerodynamic Particle Sizer or APS, Model 3321 TSI Inc., Shoreview, MN USA, respectively). At the rooftop of MO building are PM samplers: a size resolved impactor (5-stage Berner Impactor; Berner *et al.*, 1979) and a PM_{2.5} sampler (Minivol, Airmetrics, 2012). An automated weather station (AWS - Vantage Pro 2, Davis Instruments Corporation, Hayward, CA, USA) continuously measured meteorological parameters.

Aerosol Container

Roadside measurements were conducted with the aerosol container, built by TROPOS, that was equipped with instrumentation for online measurements of physical aerosol parameters and offline sampling for aerosol chemical analyses. The same inlet and drying systems used in MO UBS were also used in the aerosol container. We note that in the beginning of the campaign, the Nafion®Permapure dryers were followed by an automatic drying chamber with diffusion dryers (Tuch *et al.*, 2009) until it failed to operate on the first week of April and had to be replaced with another Nafion®Permapure dryer. Inside the aerosol container were duplicates of the instruments at MO UBS: the APS, MAAP, and MPSS. Additionally, measurements of particle volatility with a Volatility Tandem Differential Mobility Analyzer (VTDMA), eBC mass concentration with a 7-wavelength Aethalometer® Model AE33 (Magee Scientific, Berkeley, CA), and scattering coefficients with an integrating nephelometer (Aurora 4000 Model, Ecotech, Pty, Ltd, Knoxfield, Australia) were obtained.

Mobile Measurement Unit

The mobile measurement unit or the TROPOS aerosol backpack contained instruments measuring the following: total particle number concentration (condensation particle counter or Brechtel's MCPC Model 1710, Hayward, CA), particle number size distribution (optical particle size spectrometer of type TSI OPSS Model 3330) and eBC mass concentrations (microAeth® AE51 model, AethLabs, San Francisco, CA). Air is introduced at the following flow rates: 1.0, 0.4, and 0.1 L min⁻¹ for OPSS, MCPC, and AE51, respectively. The aerosol is dried using a silica-based diffusion dryer before it enters the instruments to avoid hygroscopic growth. It has been known that rapid changes in RH can result in peaks from the AE51 data, which are not related to eBC mass concentrations (Cai *et al.*, 2014).

The aerosol backpack is also equipped with a GPS unit, relative humidity and temperature sensors, and a laptop for data acquisition. Real-time data monitoring was also possible via wireless connection between the laptop inside the backpack and a smart phone.

Absorption Photometers

Measurements of eBC mass concentration were obtained from the MAAP and AE51 instruments. Descriptions and instrument parameters are listed in Table 2. For measurements at the fixed sites, eBC mass concentrations were measured using MAAP. It determines the particle light absorption coefficient by measuring the light attenuation through a particle-loaded a filter at a wavelength of 637 nm and the light reflection at two angles. From the particle light absorption coefficient, the eBC mass concentration is calculated, using a default mass absorption cross section of 6.6 m² g⁻¹ (Petzold and Schonlinner, 2004). For this campaign, TROPOS has modified the flow rate of the MAAP from 16 L min⁻¹ to 3 L min⁻¹ to avoid filter loading, when measuring at highly polluted sites (Hyvärinen *et al.*, 2013).

The eBC mass concentrations measured with MAAP were referenced to standard temperature and pressure (STP; 273 K and 1013 hPa) which are different from ambient conditions. Therefore, for comparability, an STP correction of the data according to standard values for the campaign (298 K and 1013 hPa) was performed.

For mobile measurements of eBC mass concentration, the Aethlabs microAeth® Model AE51 aboard the aerosol backpack was used. It determines the light attenuation through a particle-loaded a filter at a wavelength of 880 nm, which is then assumed as apparent absorption of eBC. The apparent absorption is interpreted as the eBC mass concentration by dividing the attenuation by the mass attenuation cross section (12.5 m² g⁻¹) given by the manufacturer. The sample flow was kept at 100 mL min⁻¹ and the time resolution was set to one second for better investigation of the spatial variability. With one-second resolution, Cheng *et al.* (2013) found high noise level at concentrations less than 2 µg m⁻³. However, a noise reduction-averaging algorithm (Hagler *et al.*, 2011) was not used in this study, since this is applicable to areas with low levels of eBC mass concentration. Processing of the one-second data to the median of every 10 seconds eliminated the noise problem. Further post processing of the AE51 data involved the STP and flow corrections. Flow rate measurements were obtained using a volumetric flow meter. Hence, the flow was corrected to standard flow to make it comparable to other instruments.

Table 2. Description of the instruments used for eBC mass concentration measurements.

Parameters	AE51	MAAP
Wavelength	880 nm	637 nm
Flow rate	0.1 L min ⁻¹	3 L min ⁻¹
Time resolution	1 s	60 s
Spot diameter	0.3 cm	1.6 cm
Mass attenuation cross section	12.5 m ² g ⁻¹	-
Mass absorption cross section	-	6.6 m ² g ⁻¹

Aethalometers, including AE51, have been known to exhibit a negative bias due to the accumulation of particles on the filter (Good *et al.*, 2016). Hence, to minimize filter-loading effects, the following measures were taken: a new filter was used for each run, the flow was kept low at 0.1 L min^{-1} , and the measurement period was limited to one hour. Repeated inter-comparisons with the reference instrument (MAAP) show that the AE51 did not demonstrate significant filter saturation (Figs. S2 and S3). Hence, a filter loading effect correction was not performed on the AE51 data to avoid over correction.

DATA AND METHODS

Quality Assurance

During the campaign, the instruments in MO UBS and aerosol container were checked daily. Every two weeks, the aerosol flow of every instrument and the main inlet system were measured to check for leaks in the system. For the aerosol container, the sample flow rates of the instruments were also checked before and after moving to a different site. The data corresponding to days when the instruments were thoroughly checked (every 2 weeks) were not included in our data analysis. In summary, there were 56 days of data processed for the MO UBS, 33 days for KAT RS, and 19 days for TAFT RS (Table 3).

Halfway through the campaign, an inter-comparison between the instruments in the aerosol container, aerosol backpack, and MO UBS was performed. The aerosol container was placed close to MO UBS but at ground level (MO GL) for 7 days. To distinguish the eBC instruments from the aerosol container and the MO UBS during the inter-comparison period, we use the following terminologies: MAAP_GL and MAAP_UBS, respectively. The MAAP_UBS were compared with the MAAP_GL (Fig. S2) and the instruments showed strong correlation with $r^2 = 0.99$ (slope = 1.00) (Fig. S3(a)).

Mobile measurements, which began and ended at MO UBS, were also done simultaneously. Comparison between the AE51 and MAAP_GL was done by selecting the data from the AE51 (1-minute averages) when it was in the urban background region (ADMU Campus) and data from MAAP_GL with the same time stamps. Strong correlation between the two instruments was found with an r^2 of 0.97 and a slope of 1.05 (Fig. S3(b)).

Mobile Measurements - Area Averaging

From the raw 1-s data of the AE51 and GPS, the median of 10-s was chosen to minimize the presence of peaks that may have been caused by single events. Next, flow correction

was applied on the data. Runs with complete information and without instrumental errors were then selected and merged into one file. The data was then categorized according to time: 2 PM weekdays (WD), 2 PM weekends (WE), 1 PM WD, 1 PM WE, 5 PM WD and 5 PM WE. This data was then plotted in a single map and GPS data points that were not in the route were removed. The result is a map with numerous data points concentrated on the chosen route.

Since the GPS data points from the multiple runs were not exactly at the same place at the same time, averaging has to be done spatially. Using the latitude, longitude, and eBC mass concentration of the cleaned data, the aim was to create squares along the route, and to average the eBC mass concentrations that lie within the square. This procedure required center points, which are, composed of a pair of latitude and longitude data. The chosen center points were created using QGIS 6.4.4. The route was drawn on a map as a vector layer. Equidistant center points along the route were created, in this case, the distance between two points was approximately 5.6 m. Different distances were tried and with this value, the high-resolution data was still captured. Then, the coordinates of the equidistant points were used as center points for area averaging.

The area averaging, which was performed in IGOR Pro 6.3 (WaveMetrics, Portland, OR), required the following parameters: latitude, longitude, BC concentration, center points X and Y, and a fifth variable, which we designate as the “side length”. The side length determines the dimension of the square for area averaging. To maintain the high resolution data, the side length was set to 22.3 m, therefore the area being averaged is $\sim 50 \text{ m}^2$. This area is larger than the distance between two center points; therefore, there were overlaps in the averaging. Consequently, the results are moving area averages of eBC mass concentration along the route. This averaging was performed on all the squares in the route. The result is one spatial plot showing the average of all the mobile runs with high spatial resolution.

Background Correction

The spatial distribution was stratified per zone: green zones, normal zones, and hotspots. The green zones were defined as areas with mean eBC mass concentrations lower than $10 \mu\text{g m}^{-3}$ since concentrations in Metro Manila were observed to be elevated. Other parts of the route with increasing mean concentration and variability were categorized as the “normal zones” and “hotspots” (Fig. 3). The green zones are private areas, areas with open spaces, characterized by the presence of trees, and are not open to public vehicles. The normal zones are areas with flowing traffic and footbridges. The hotspots are areas with PUV

Table 3. Descriptive statistics of eBC mass concentrations at the different measurements sites.

Station	# of days	eBC mass concentration in $\mu\text{g m}^{-3}$			
		mean	standard deviation	median	25 th –75 th percentile
MO UBS	56	6.9	4.8	5.9	3.4–9.2
KAT RS	33	16.5	11.7	13.4	7.9–21.8
MO GL	7	7.6	4.9	6.8	4.2–10.2
TAFT RS	19	25.7	17.2	21.3	11.3–38.6

terminals, intersections with traffic light, idle cars, and pedestrians. These are also zones with street canyons and other complex street topographies. Normal zones and hotspots are more difficult to define quantitatively due to the observed high variability in the eBC mass concentrations in these areas. Stratifying the data per zone eases the analysis of background correction.

The measured eBC mass concentration is a combination of contributions of local component and background component. Hence, to determine the contribution of the local component, the background component may simply be subtracted from the observed concentration (Lenschow *et al.*, 2001). However, in this study, the fixed urban background station may still be influenced by nearby traffic sources. Hence, the pragmatic approach introduced by Van Poppel *et al.* (2013) was used in this study wherein the background concentration was estimated from the mobile measurements using the lower percentiles of the observed eBC mass concentrations along a part of the route with the lowest traffic density. However, in this study, nearly half of the route is within the urban background region where some parts are completely away from traffic source (park and campus areas). The average of the eBC mass concentrations ($4.78 \mu\text{g m}^{-3}$) measured at these regions were used as an estimation of the background concentrations. The background concentration value obtained is comparable to BC (OC+EC) measured at a rural site ~50 km away from the metropolitan area ($\sim 6.3 \mu\text{g m}^{-3}$; higher due to contribution of OC) as reported by Bautista *et al.* (2014).

To compute for the contribution of local sources to ambient eBC mass concentration, the equation below was used:

$$\text{local contribution} = \frac{eBC_{UN} - eBC_C}{eBC_{UN}} \quad (1)$$

where, eBC_{UN} is the uncorrected eBC value and eBC_C is the background corrected eBC value. Due to the proximity of the measurement sites and routes to major roadways, eBC measurements were significantly influenced by vehicular traffic. Hence, it is possible to assume that the local sources are mostly traffic-related, although other sources such as open cooking should also be considered.

RESULTS AND DISCUSSION

Diurnal Variability of eBC Mass Concentrations

Fig. 4 shows the diurnal variability of eBC mass concentration and particle number concentration from 30 nm–300 nm ($PNC_{30-300\text{nm}}$, size range of soot particles) measured from MO UBS and the aerosol container at KAT RS and TAFT RS. Mean, standard deviation, median, and 25th–75th percentiles of eBC mass concentrations are provided in Table 3. The highest mean eBC mass concentration and variability were observed at TAFT RS ($25.7 \pm 17.2 \mu\text{g m}^{-3}$) while the lowest mean was measured at MO UBS ($6.9 \pm 4.9 \mu\text{g m}^{-3}$). KAT RS has a mean eBC mass concentration of $16.5 \pm 11.7 \mu\text{g m}^{-3}$, about two times higher than at MO UBS.

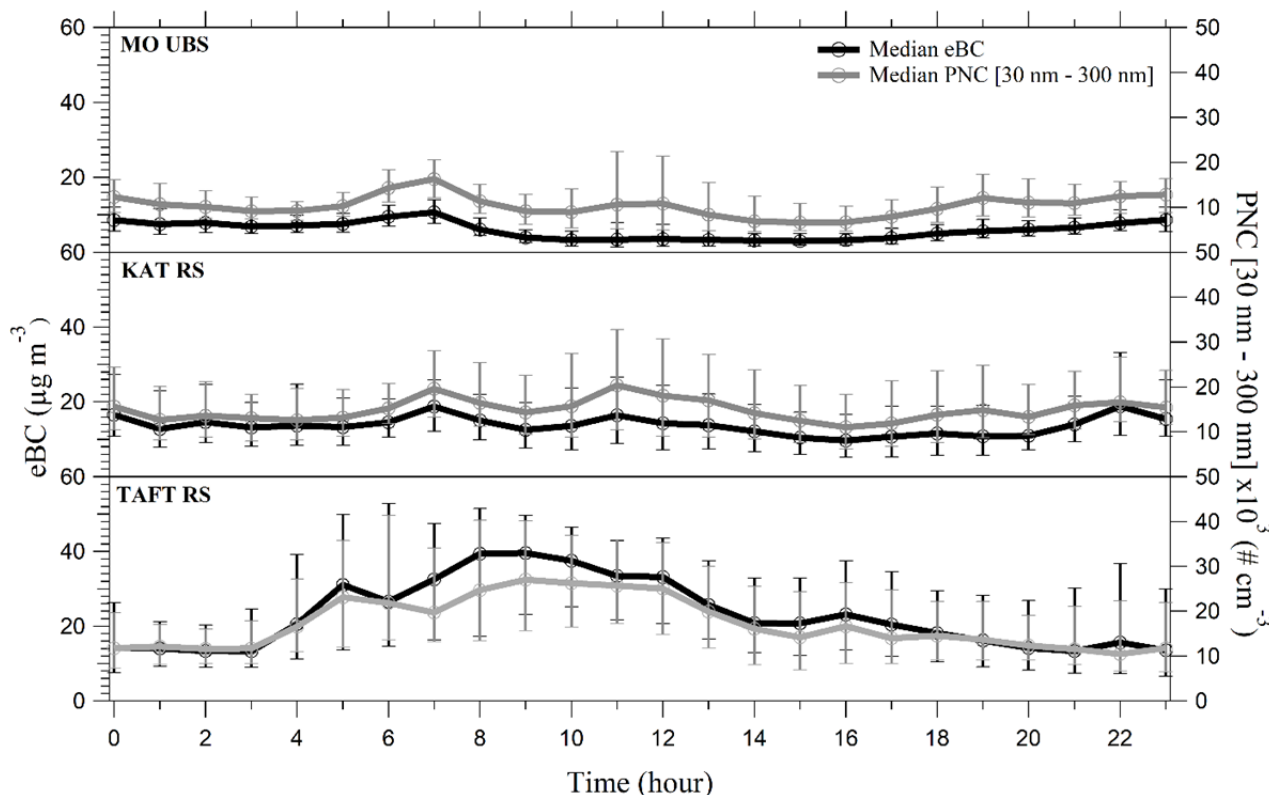


Fig. 4. Statistical summary (median, 25th and 75th percentiles) of the diurnal cycle eBC mass concentration (black) and particle number concentration from 30 nm–300 nm (grey) for MO UBS (top), KAT RS (middle), and TAFT RS (bottom).

Diurnal analysis at the roadside showed higher short-term variability, as expected, than in the urban background regions. The roadside sites are closer to traffic sources; they are more susceptible to turbulent winds caused by each passing vehicle.

Diurnal trends of eBC mass concentrations and $\text{PNC}_{30-300\text{nm}}$ are comparable across all measurement sites. Similar to eBC, the lowest $\text{PNC}_{30-300\text{nm}}$ was measured at MO UBS, followed by KAT RS, and the highest at TAFT RS. The average particle number size distribution (PNSD) illustrated in Fig. S4 also shows similar results. For MO UBS and KAT RS, the PNSD during the day (4:00–16:00), when humans are more active, has no significant difference from the 24 hour average. However, for TAFT RS, the daytime PNSD is higher than the 24 hour average from 10 nm to 800 nm. This implies that eBC mass concentrations measured at all sites are in the fine mode and PNSD in a street canyon exhibits a significant influence of human activities during daytime. Further analysis on the factors that influence these diurnal patterns are in the following sections.

Diurnal Variability of eBC Mass Concentration at the Urban Background Area

At MO UBS, the peaks were observed in the morning (7:00 AM) and late in the evening (11:00 PM). On the other hand, lower concentrations were observed during the day from 10:00 AM to 5:00 PM. Different studies (Babu *et al.*, 2002; Beegum, *et al.*, 2005; Tripathi *et al.*, 2005; Mahalakshmi *et al.*, 2011; Kompalli *et al.*, 2014) investigated the relationship between eBC and the dynamics of the local atmospheric boundary layer, particularly in tropical regions. The common observation is that eBC mass concentrations peak a few hours after sunrise and sunset, and are low during the afternoon. In Fig. 4 (top panel), we see a peak in the morning at MO UBS (6:00 AM–9:00 AM) with eBC mass concentrations around $10 \mu\text{g m}^{-3}$ which can be a result of both fumigation effect and human activities. Then the concentration decreases ($\sim 3\text{--}6 \mu\text{g m}^{-3}$) between 9:00 AM–5:00 PM. As the temperature increases during the day, the depth of the mixing layer increases due to thermal convection and aerosol particle concentrations decrease. This decrease is enhanced by generally stronger winds in the afternoon. The eBC mass concentration increases again after sunset (6:30 PM–7:30 PM), since the vertical convection decreases and the boundary layer settles. This concentration remains until it begins to decrease again at dawn. A different diurnal behaviour is observed for the eBC mass concentration at both roadside sites.

Diurnal Variability of eBC Mass Concentration at Roadside Sites

At KAT RS, high concentrations were observed at 7:00 AM. However, the peak at noon and high concentrations in the afternoon is opposite to that of MO UBS. Furthermore, there is a sharp increase in concentration from 9:00 PM. Conditional probability function (CPF) analyses were performed to determine the direction of source contributions to eBC mass concentrations. Fig. 5 presents the CPF analyses for all sites where the number of events with a concentration

greater than 75th percentile is plotted as function of both wind speed and direction. At KAT RS (Fig. 5(a)), the lowest and highest source contributions for eBC mass concentrations came from the East and West, Southwest, respectively. As previously described, west of the aerosol container was the Katipunan Avenue and southwest of the aerosol container is the intersection of four major roads: Katipunan Avenue, Aurora Boulevard, Bonifacio Avenue and Marcos Highway, where traffic lights and idling cars, a jeepney terminal, and PUV stops were located. East of the aerosol container was the university campus, which has restricted vehicular access and open green spaces. Fig. 6(a) shows the CPF analysis of the wind speed and direction with respect to time of day. Stronger winds originating from SW were observed from 12:00 PM to 8:00 PM—which is mostly the time when trucks are allowed on the road. Therefore, this high eBC mass concentration may be due to both the activities in this intersection and the presence of trucks entering Katipunan Avenue during this time of the day. This result suggests that traffic reducing schemes such as the Truck Ban policy do not necessarily equate to an improvement in air quality. In this case, the eBC mass concentration even increased. Latha and Badarinath (2005) have studied impacts of truck emissions on the BC mass concentration in India. They performed measurements during a nationwide truck strike where BC gradually decreased by 15%, but abruptly increased the moment the strike ended. Since, we do not see a sudden decrease and increase in eBC mass concentration before and during the truck ban window, it may imply that the trucks are not the only major source of eBC at this site. In another study under MACE 2015 by Kecorius *et al.* (2017) focusing on TAFT RS, it was found that jeepneys, which is only 20% of the total vehicle fleet, is responsible for 94% of the soot particle mass. Katipunan Avenue is also frequented by jeepneys and the results of Kecorius *et al.* (2017) suggests that aside from trucks, jeepneys contribute to eBC emissions.

TAFT RS, on the other hand, shows a different trend (Fig. 4 bottom panel). Within the day, eBC mass concentrations increase between 5:00 AM–12:00 PM and decrease from 12:00 PM–4:00 PM, probably due to thermal convection. A second eBC mass concentration peak is observed from 5:00 PM–6:00 PM with a decrease after midnight to approximately $10 \mu\text{g m}^{-3}$. CPF analysis (Fig. 5 (b)) shows that elevated eBC mass concentrations originated from the North and East. Referring to the location of the aerosol container, the Taft Avenue runs from Northwest to Southeast. Higher wind speeds (Fig. 6(b)) at this location are mostly from West Southwest in the afternoon, which corresponds to the general direction of the Manila Bay, while lower wind speeds originate from the North and East. We think that the strong sea breeze from the Manila Bay together with convection may be responsible for decreasing eBC mass concentrations in the afternoon. On the other hand, when there are lower wind speeds, there is little ventilation in the area for the emissions to be dispersed or transported to other locations. The street canyon configuration of Taft Avenue further inhibit the ventilation of air. Hence, vehicle emissions tend to accumulate in the

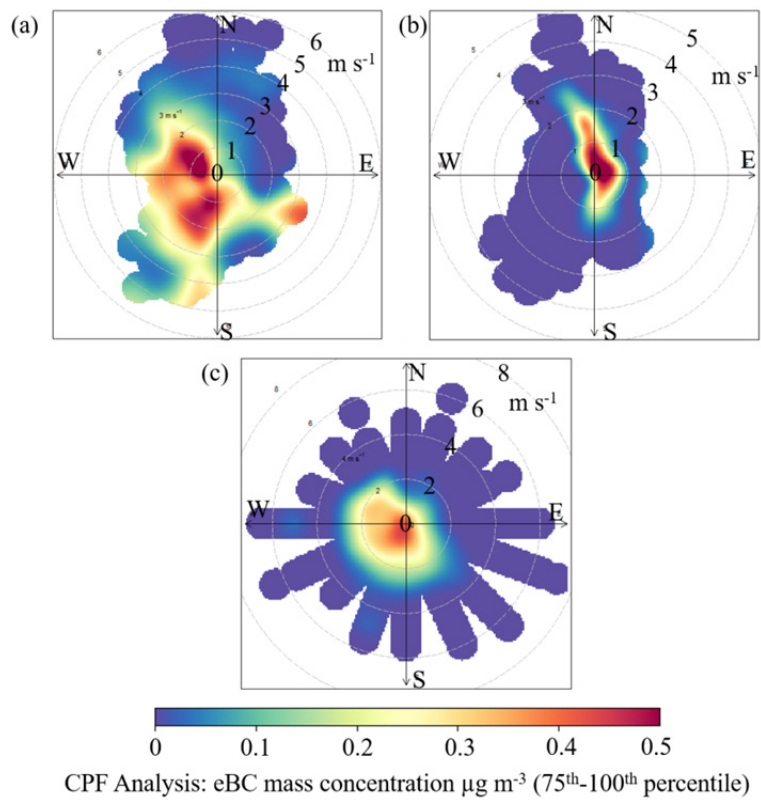


Fig. 5. CPF Analysis of the 75th–100th percentiles of eBC mass concentrations at (a) KAT RS, (b) TAFT RS and, (c) MO UBS with wind direction and wind speed, represented by the radius, measured at the top of the container (for Katipunan and Taft) and on the rooftop of a building at MO UBS.

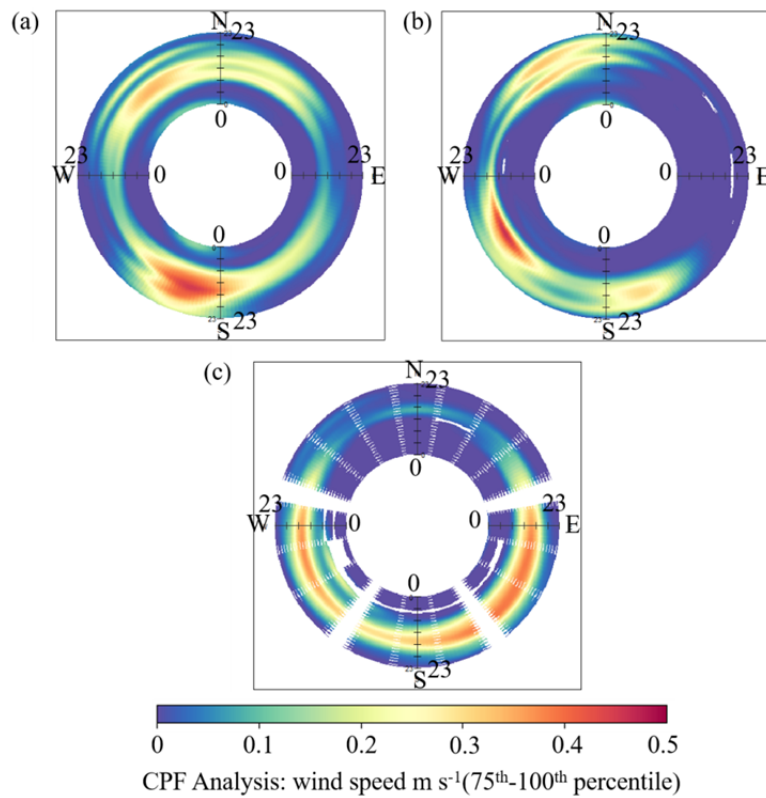


Fig. 6. CPF analysis of high wind speeds (75th–100th percentiles) for different times of the day (radius) at (a) KAT RS, (b) TAFT RS, and (c) MO UBS.

area. Furthermore, although trucks are not allowed along Taft Avenue (Manila section), this road is frequented by private and public vehicles (jeepneys). As mentioned above, results of Kecorius *et al.* (2017) gives evidence on the contribution of jeepney emissions on the eBC mass concentration along Taft Avenue. These factors contribute to the higher eBC mass concentrations observed at this location, which have been reported in previous studies performed in similar street configurations (Boogaard *et al.*, 2011; Van Poppel *et al.*, 2013; Rakowska *et al.*, 2014).

A study in New York by Lena *et al.* (2002) showed that the mean elemental carbon (EC) concentration at a no-truck-traffic residential area is $2.6 \mu\text{g m}^{-3}$, which is around three times lower than the mean eBC mass concentration at MO UBS. While at a traffic route, the mean EC is $7.3 \mu\text{g m}^{-3}$, about two to three times lower than Taft and Katipunan roadside eBC mass concentrations. The mass concentration of eBC during the Truck Ban window hours almost doubles relative to the times when trucks are not allowed on the road. Diurnal variation of the eBC mass concentration at the urban background region shows their dependency on the meteorology, in terms of atmospheric boundary layer, and traffic sources. However, we also found that closer to the traffic source, eBC mass concentrations are less influenced by the evolution of the boundary layer and more influenced by traffic emissions, Truck Ban window hours (at KAT RS), topographic profile (TAFT RS), and wind direction, as compared to an urban background region.

As mentioned before, Hopke *et al.* (2008) showed that the Philippines has the second highest BC among Asian countries with daily means at MO ground level ranging from 0 to $\sim 90 \mu\text{g m}^{-3}$ with a median of ~ 12 to $15 \mu\text{g m}^{-3}$ from 2002 to 2005. The daily mean of the eBC mass concentration obtained during Stage 2 of the campaign (MO ground level) for 7 days ranged from ~ 5 to $10 \mu\text{g m}^{-3}$ with a median value of approximately $8 \mu\text{g m}^{-3}$. It might seem like there is a decrease in eBC mass concentration this year but note that the sampling duration of Hopke *et al.* (2008) covers all seasons (both dry and wet) from year 2002 to 2005, while for this study it was only 7 days during the dry season. Furthermore, the reflection method used in Hopke *et al.* (2008) has larger uncertainties for dark filter samples.

In comparison, daily median eBC mass concentrations measured at the three sites in this study are comparable with other roadside and urban areas in Asian cities, albeit slightly more elevated. For example, levels at MO UBS were similar to levels at a roadside station in Seoul, Korea (Lee *et al.*, 2007) and an urban area in Beijing, China (Song *et al.*, 2015). At KAT RS, eBC mass concentrations were comparable with a roadside station in Bangkok, Thailand (Hung *et al.*, 2014) and an urban area in Xi'an, China (Cao *et al.*, 2009). At TAFT RS, however, eBC mass concentrations were significantly elevated, and is up to 30 times higher when compared with roadside sites in European cities with a Low Emission Zone (e.g., Leipzig, Germany) (Birmili *et al.*, 2015).

Spatial Variability of eBC Mass Concentration

The mobile measurements at the Katipunan area started

in the middle of March and ended in mid-May. After data selection, the total number of runs in Katipunan was 77 of which 55 were weekday runs and 22 were weekend runs. Due to the occurrence of rain events and shorter measurement period, the total number of runs in the Taft area were only 34 of which 25 were weekday and 8 were weekend runs. Fig. 7 shows the spatial plot of the mean BC concentrations obtained from all mobile measurements along Katipunan and Taft routes.

Katipunan

Fig. 7(a) shows the spatial distribution of eBC mass concentration along the Katipunan route. The lowest mass concentrations (~ 3 to $15 \mu\text{g m}^{-3}$) were found inside the ADMU campus and in the residential area west of the route. Higher mass concentrations were found along Katipunan Avenue and on the streets parallel and perpendicular to it. The highest mean value ($75.7 \mu\text{g m}^{-3}$) was observed at the southern part of the route, which is a terminal station of diesel-powered PUVs or jeepneys, next to a major intersection of four roads. All the green zones have mean eBC mass concentrations below $10 \mu\text{g m}^{-3}$. The mean eBC mass concentration in the green zones (G1–G6) over all the runs done at 2:00 PM and 5:00 PM is $5.7 \pm 1.5 \mu\text{g m}^{-3}$, which is comparable with the hourly mean value of $6.9 \pm 4.4 \mu\text{g m}^{-3}$ obtained at the MO UBS site. These zones also have the lowest variability. On average, the eBC mass concentrations at the normal zones ($14.1 \pm 2.5 \mu\text{g m}^{-3}$) are 2.5 times higher than in the green zones. While in the hotspots, the mean eBC mass concentration is $34.6 \pm 13.8 \mu\text{g m}^{-3}$, which is higher by a factor of 2.5 and 6 than the normal and green zones, respectively. This relative high concentration is due to the proximity of the hotspots to traffic sources. The hotspots are areas with jeepney terminals, main roads with heavy traffic, and major intersections. The highest mean eBC mass concentration over all runs was measured at H1 ($58 \mu\text{g m}^{-3}$). H1 is a populous area with street vendors, terminal operators, barkers, and police/traffic officers working in the area for at least eight hours a day. This area is also under a flyover with a high-rise building on the east. With this infrastructure, there is little ventilation, and therefore, low chance for the emissions to be dispersed. Furthermore, the particulate emissions may also accumulate because H1 has traffic sources from all sides (cars can also pass in between the terminals).

Mobile measurements were conducted at two different times of the day, for both weekdays and weekends. Fig. S5(a) shows the comparison of eBC mass concentrations in each zone between the 2:00 PM and 5:00 PM runs, which are represented by the black and grey bars, respectively. The error bars represent the standard deviation. Results show that at 5:00 PM, eBC mass concentration is higher in the green zones and other parts of the route than at 2:00 PM. This is due to the increase of vehicular emissions during the evening rush hour. However, along Katipunan Avenue, there are parts where eBC mass concentrations at 2:00 PM is higher than at 5:00 PM (H3–H5). This is because these zones are much closer to the main road that is filled with trucks during Truck Ban window hours.

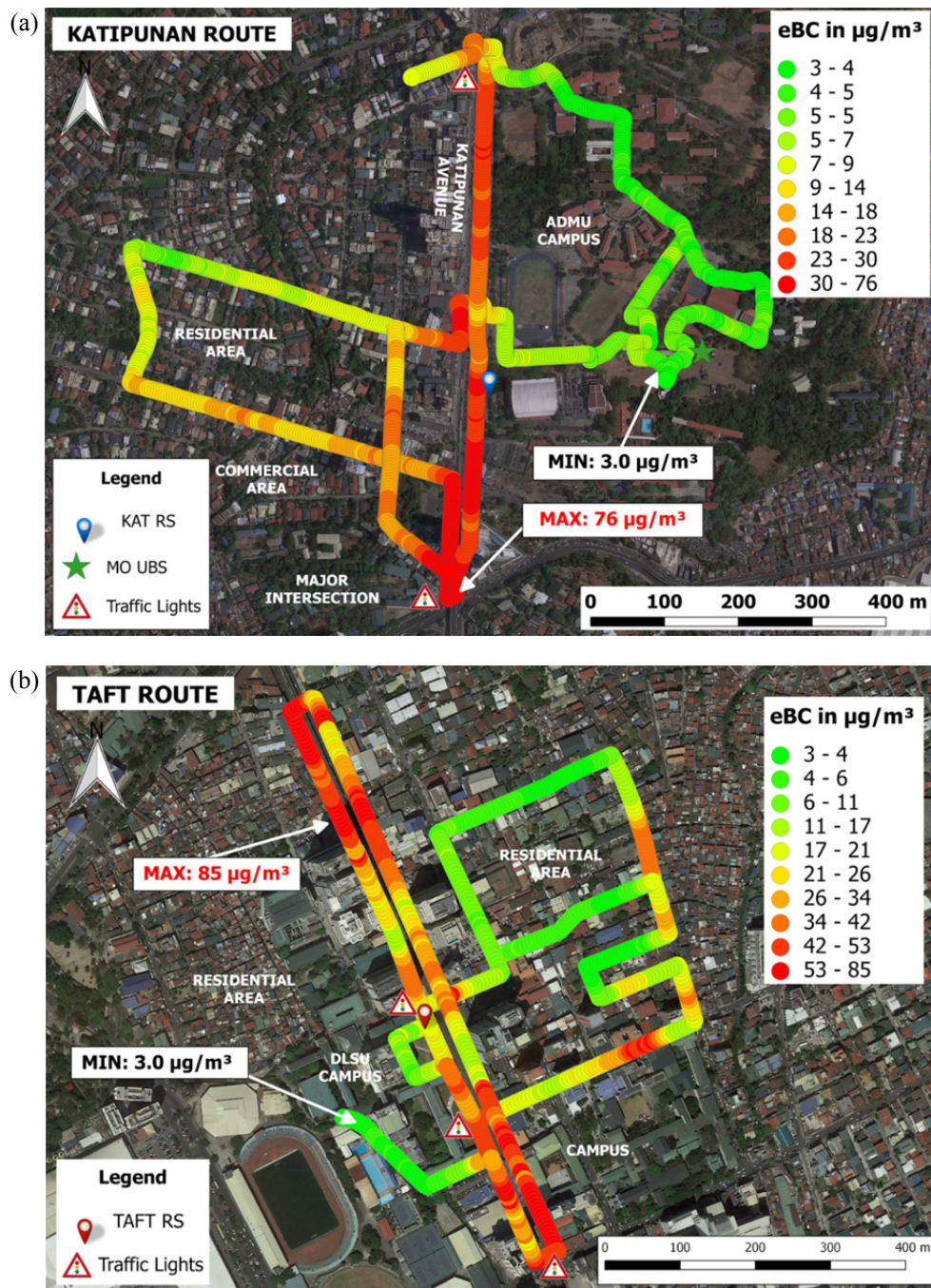


Fig. 7. Spatial distribution of eBC mass concentrations along Katipunan Route (a) and Taft Route (b).

Fig. S5(b) shows eBC mass concentrations during the weekdays (black) and weekends (grey). In the urban background region (ADMU campus) the mean eBC mass concentrations of zones G1–G4 have little difference between each other. However, for residential areas G5 and G6, a $2\text{--}4 \mu\text{g m}^{-3}$ difference was observed. In the normal zones, the eBC mass concentrations is higher during the weekdays than during the weekends. We note that in the hotspot areas, the eBC mass concentration is more variable. In H2 and H3, weekend eBC mass concentration is higher than during weekdays.

Further analysis also revealed that in most zones, the

eBC mass concentrations are higher during weekdays than during the weekends. However, the eBC mass concentrations are higher in some hotspots during the weekends. A possible explanation is that the Truck Ban Policy and the Number Coding for vehicles are lifted and all vehicles are allowed to use the roads over the weekend.

Taft

Fig. 7(b) shows the eBC mass concentrations along the Taft Route. Elevated mass concentrations were measured at the main roads and with a maximum close to an intersection. On the other hand, lower concentrations were found in the

narrow streets not passable by vehicles and inside DLSU campus. However, two of the green zones that are close to Taft Avenue have values exceeding $10 \mu\text{g m}^{-3}$. This is due to the proximity of these zones (G2 and G3) to the traffic sources. In addition, there is no real urban background region in Taft as this is a highly urbanized area. Nevertheless, the lowest eBC mass concentration was still observed further inside the DLSU campus, and the mean eBC mass concentration in all green zones was $7.7 \pm 3.8 \mu\text{g m}^{-3}$. In the normal zones, the eBC mass concentrations are three times higher than at the green zones, and also with higher variability ($24.3 \pm 6.6 \mu\text{g m}^{-3}$). The hotspots, as expected, have the highest concentrations with a mean value of $43.3 \pm 7.1 \mu\text{g m}^{-3}$, which is two times higher than the normal zones and seven times greater than the green zones. The highest concentrations were found at both ends of the route, which are train stops. These train stops exhibit a “tunnel-like” characteristic. Underneath these train stations are traffic lights. Therefore, the concentration maybe attributed to the poor dilution of aerosols and traffic regime.

Two runs a day were also conducted in this route, one at 1:00 PM and another at 5:00 PM. Fig. S5(c) shows the comparison between these two time periods. In all zones, BC levels at 5:00 PM are higher than at 1:00 PM. This was expected since at 1:00 PM, most people are at work or in school, and 5:00 PM is the evening rush hour. In Fig. S5(d), eBC mass concentration were also compared for weekdays and weekends. In most zones, eBC mass concentrations were higher during the weekends than during the weekdays. Due to the limited number of runs, this high value may not be representative of the investigated period. The complexity of the street configuration around the Taft area made categorizing of the route into zones more challenging. Particularly, the lack of a meteorological instrument aboard the backpack or in specific parts of the route made it challenging to study the effects of ventilation to eBC mass concentrations. The occurrence of rain events resulting to limited number of runs also added to the difficulty of the analysis – making this part of the study inconclusive.

A comparison of the Katipunan and Taft's eBC spatial distributions showed that the eBC mass concentration in Taft is on average is higher by a factor of 1.5 compared to the Katipunan area. Katipunan Avenue may have more lanes, but the area is relatively open. On the other hand, Taft Avenue has fewer lanes but is characterized by a street canyon configuration. The spatial analysis of two different routes shows the dependency of the street level eBC mass concentration on proximity to traffic source, traffic regime, vehicle type, and street configuration. It also shows that eBC mass concentration varies significantly within a 500-m radius. Thus, this study shows that high-resolution mobile measurements are able to examine the heterogeneity of eBC mass concentrations and the factors that drive it, which is not possible with fixed measurements alone.

Table 4 summarizes the eBC mass concentrations measured at the different zones for each route. Comparing the two routes, eBC mass concentration along the Taft route is higher and more variable than along the Katipunan route. In comparison, these eBC mass concentration values

Table 4. Summary of the eBC mass concentrations in $\mu\text{g m}^{-3}$ (mean \pm sd) measured at the different zones for both Katipunan and Taft routes.

Zones	Katipunan	Taft
Green zones	5.7 ± 1.5	7.7 ± 3.8
Normal zones	14.1 ± 2.5	24.3 ± 6.6
Hotspots	34.5 ± 13.8	43.3 ± 7.1

obtained in two key areas in Metro Manila are notably higher than the reported values of mobile measurements conducted in other countries using the same instrument (AE51). In Belgium, for example, the median values of eBC mass concentration were determined to be $3 \mu\text{g m}^{-3}$ and $6 \mu\text{g m}^{-3}$ at a background zone and in higher traffic density areas, respectively (Van Poppel *et al.*, 2013). A study done at Braunschweig, Germany showed that at an urban park site, eBC was only $1.4 \mu\text{g m}^{-3}$ while eBC was $4.1 \mu\text{g m}^{-3}$ at a curb side spot (Ruths *et al.*, 2014). In California, Westerdahl *et al.* (2005) reported that eBC mass concentrations at residential areas range from 0.7 – $1.5 \mu\text{g m}^{-3}$ and $12 \mu\text{g m}^{-3}$ at the freeway. The eBC mass concentration in the green zones in this study are two to five times higher, while they are five to ten times higher in the hotspot areas compared to the corresponding regions in the various previous studies.

Background Correction

The mean of the green zones (G1–G4 only) from the Katipunan route was subtracted from the entire data set for background correction. Fig. S6 shows the estimation of the urban background concentration from each zone for the Katipunan route (Fig. S6(a)) and Taft route (Fig. S6(b)). Here we see that the influence of the local contributions increased as we move from the green zones to normal zones and finally the hotspots. Fig. 8 shows the contribution of local sources for both routes. In the Katipunan route, the local sources contributed 0–40%, 55–75%, and 77–92% of ambient eBC mass concentrations in the green zones, normal zones, and hotspots, respectively. On the other hand, the contributions were higher in the Taft area with percentages ranging from 8–65%, 70–87% and 88–91% at the green zones, normal zones and hotspots, respectively. This suggests that the eBC mass concentrations at green zones along both routes were relatively uniform although green zones closer to streets were highly influenced by local sources, which can be assumed to be traffic-related. For the normal zones, after background correction, the local sources contributed 50–80% to the total observed eBC mass concentration. The hotspots, however, remain higher than the other zones, indicating that due to the proximity of these zones to the road, the major contributors are the local traffic sources (80–90%). Comparing the normal zones of the two routes, local sources have a higher contribution to the ambient air quality in Taft than in Katipunan. However, for the hotspots, the local contributions are similar. Therefore, different streets in certain locations are affected differently by local sources. This result shows that the contribution of local sources in a megacity is also heterogeneous.

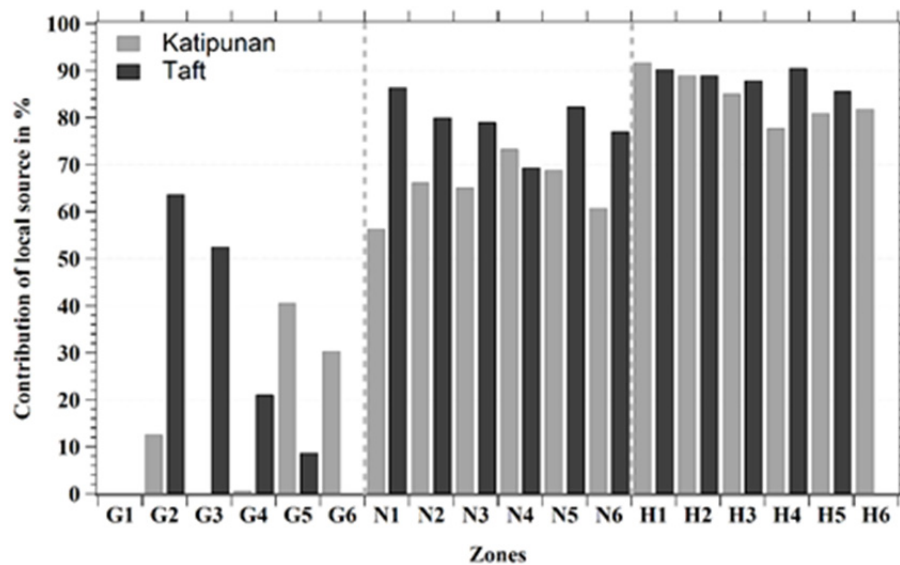


Fig. 8. Summary of the contributions of local sources to eBC mass concentration in ambient air for each zones of (grey) Katipunan Route and (black) Taft Route computed using Eq. (1). The background concentration was estimated from the zones G1-G4 of the Katipunan Route.

CONCLUSIONS

In this study, we present the spatial and diurnal variability of equivalent black carbon (eBC) mass concentration in the megacity of Metro Manila, Philippines in the summer of 2015. Fixed measurements were performed in an urban background station and two subsequent roadside sites. Mobile measurements were conducted along two fixed routes with an instrumented backpack.

Diurnal analysis of eBC mass concentrations showed that urban background region was mainly influenced by the dynamics of the local boundary layer while at the roadside site only 300 m away, the main factors at play were vehicle fleet and volume, traffic scheme, and street topography. This study also documented, from a comparison of the two roadside sites, that although there were heavy-duty trucks in the wide-open roadway, eBC mass concentrations recorded on its roadside are much lower than in a narrow street canyon. This gives evidence to the notion that policies made to ease traffic volume do not necessarily improve air quality, and in some instances, as shown in this study, such policies seem to worsen it. Furthermore, to our knowledge, such complex street configuration (street canyon with elevated railway) has never been profiled before and needs to be further studied to increase our understanding of the pollutant dynamics, ultimately reducing the uncertainties of climate and exposure models.

Mobile measurements proved to be extremely advantageous in capturing the spatial distribution of eBC mass concentration in different microenvironments. The spatial analysis revealed high heterogeneity of eBC mass concentrations, ranging from 3–80 $\mu\text{g m}^{-3}$ within a 500-m radius. Highest concentrations were found in crowded areas where people are stay for more than 8 hours a day. Result from this study is about ten times higher than previously reported from European (Van Poppel *et al.*, 2013; Peters *et*

al., 2014; Ruths *et al.*, 2014; Klompmaker *et al.*, 2015) and US sites (Westerdahl *et al.*, 2005), and 2 to 5 times higher than in other Southeast Asian megacities (Hung *et al.*, 2014; Rakowska *et al.*, 2014; Kim *et al.*, 2015). This sheds some light on the different air quality challenges that megacities from developing and emerging countries experience. For example, $\text{PM}_{2.5}$ in cities in China, Vietnam, Pakistan, Malaysia and India are higher than in Metro Manila. However, eBC mass concentration in Metro Manila is higher than values reported in those cities (Hopke *et al.*, 2008). This shows the advantage of using eBC mass concentration as a parameter, in addition to PM, when investigating traffic-related air pollution.

These results can help improve the analysis of health effects of air pollution, improve exposure models, validate models of spatial distribution of pollutants, and raise awareness on the increasing threat of poor air quality. Ultimately, the results presented here together with other studies related to MACE 2015 are valuable for managing air quality in megacities like Metro Manila. By creating and implementing existing policies on traffic-related air pollution, considering air pollution dynamics in urban planning, and investing on automated, real-time instruments that monitor air pollution, improvements on urban air quality are not impossible.

ACKNOWLEDGEMENTS

We acknowledge the support given by the following institutions and agencies who paved the way for this campaign to push through: Leibniz Institute for Tropospheric Research, Researchers for Clean Air Inc., Partnership for Clean Air Inc., The Manila Observatory, Ateneo de Manila University, De La Salle University, City Office of Manila, and Metro Manila Development Authority. We also recognize the support of Mr. Alberto Suansing, Mr. Renato

Pineda, and Ms. Juliet Manlapaz. Edgar Vallar and Maria Cecilia Galvez acknowledges CHED for COE research grants. Mylene Cayetano recognizes the support of the Ministry of Science, ICT and Future Planning in South Korea through the International Environmental Research Center and the UNU & GIST Joint Programme on Science and Technology for Sustainability in 2015. We are also grateful to Evelyn Gayle Tamayo and Leizel Mandueño, who are part of the main group responsible for the operation of the stations. Finally, we acknowledge all the students, professors, friends, and family members who volunteered for the mobile measurements.

SUPPLEMENTARY MATERIAL

Supplementary data associated with this article can be found in the online version at <http://www.aaqr.org>.

REFERENCES

- Adams, H., Nieuwenhuijsen, M., Colvile, R., Older, M. and Kendall, M. (2002). Assessment of road users' elemental carbon personal exposure levels, London, UK. *Atmos. Environ.* 36: 5335–5342.
- Ateneo Traffic Group (2012). Towards efficient mobility in a sustainable campus.
- Babu, S.S. and Moorthy, K.K. (2002). Aerosol black carbon over a tropical coastal station in India. *Geophys. Res. Lett.* 29: 2098.
- Bautista, A.T., Pabroa, P.C., Santos, F.L., Racho, J.M. and Quirit, L.L. (2014). Carbonaceous particulate matter characterization in an urban and a rural site in the Philippines. *Atmos. Pollut. Res.* 5: 245–252.
- Beegum, S., Moorthy, K., Babu, S., Satheesh, S., Vinoj, V., Badarinath, K., Safai, P., Devara, P., Singh, S., Vinod, Dumka, U. and Pant, P. (2009). Spatial distribution of aerosol black carbon over India during pre-monsoon season. *Atmos. Environ.* 43: 1071–1078.
- Berner, A., Lürzer, C., Pohl, F., Preining, O. and Wagner, P. (1979). The size distribution of the urban aerosol in Vienna. *Sci. Total Environ.* 13: 245–261.
- Birmili, W., Rehn, J., Vogel, A., Boehlke, C., Weber, K., and Rasch, F. (2013). Micro-scale variability of urban particle number and mass concentrations in Leipzig, Germany. *Meteorolog. Z.* 22: 155–165.
- Birmili, W., Weinhold, K., Rasch, F., Sonntag, A., Sun, J., Merkel, M., Wiedensohler, A., Bastian, S., Schladitz, A., Löschau, G., Cyrus, J., Pitz, M., Gu, J., Kusch, T., Flentje, H., Quass, U., Kaminski, H., Kuhlbusch, T.A.J., Meinhardt, F., Schwerin, A., Bath, O., Ries, L., Gerwig, H., Wirtz, K. and Fiebig, M. (2016). Long-term observations of tropospheric particle number size distributions and equivalent black carbon mass concentrations in the German Ultrafine Aerosol Network (GUAN). *Earth Syst. Sci. Data* 8:355–382.
- Boogaard, H., Kos, G.P.A., Weijers, E.P., Janssen, N.A.H., Fischer, P.H., van der Zee, S.C., de Hartog, J.J. and Hoek, G. (2011). Contrast in air pollution components between major streets and background locations: Particulate matter mass, black carbon, elemental composition, nitrogen oxide and ultrafine particle number. *Atmos. Environ.* 45: 650–658.
- Cai, J., Yan, B., Zhang, D., Kinney, P.L., Perzanowski, M.S., Jung, K., Miller, R. and Chillrun, S.N. (2014). Validation of MicroAeth® as a black carbon monitor for fixed-site measurement and optimization for personal exposure characterization. *Aerosol Air Qual. Res.* 14: 1–9.
- Cao, J.J., Zhu, C.S., Chow, J.C., Watson, J.G., Han, Y.M., Wang, G.H., Shen, Z.X. and An, Z.S. (2009). Black carbon relationships with emissions and meteorology in Xi'an, China. *Atmos. Res.* 94: 194–202.
- Chen, T. and Chen, J. (1995). An observational study of the South China Sea monsoon during the 1979 summer: Onset and life cycle. *Mon. Weather Rev.* 123: 2295–2318.
- Cheng, Y. and Lin, M. (2013). Real-time performance of the microAeth® AE51 and the effects of aerosol loading on its measurement results at a traffic site. *Aerosol Air Qual. Res.* 13: 1853–1863.
- Dons, E., Panis, L.I., Poppel, M.V., Theunis, J., Willems, H., Torfs, R. and Wets, G. (2011). Impact of time-activity patterns on personal exposure to black carbon. *Atmos. Environ.* 45: 3594–3602.
- Dons, E., Panis, L.I., Poppel, M.V., Theunis, J. and Wets, G. (2012). Personal exposure to Black Carbon in transport microenvironments. *Atmos. Environ.* 55: 392–398.
- Dons, E., Temmerman, P., Poppel, M.V., Bellemans, T., Wets, G. and Panis, L.I. (2013). Street characteristics and traffic factors determining road users' exposure to black carbon. *Sci. Total Environ.* 447: 72–79.
- Dons, E., Van Poppel, M., Int Panis, L., De Prins, S., Berghmans, P., Koppen, G. and Matheeuissen, C. (2014). Land use regression models as a tool for short, medium and long-term exposure to traffic related air pollution. *Sci. Total Environ.* 476–477: 378–386.
- Ghassoun, Y., Ruths, M., Löwner, M. and Weber, S. (2015). Intra-urban variation of ultrafine particles as evaluated by process related land use and pollutant driven regression modelling. *Sci. Total Environ.* 536: 150–160.
- Good, N., Mölter, A., Peel, J.L. and Volckens, J. (2016). An accurate filter loading correction is essential for assessing personal exposure to black carbon using an Aethalometer. *J. Exposure Sci. Environ. Epidemiol.* 27: 409–416.
- Hagler, G.S., Yelverton, T.L., Vedantham, R., Hansen, A.D. and Turner, J. R. (2011). Post-processing method to reduce noise while preserving high time resolution in Aethalometer real-time black carbon data. *Aerosol Air Qual. Res.* 11: 539–546.
- Health Effects Institute (HEI) (2010). *Traffic-related air pollution: A critical review of the literature on emissions, exposure, and health effects*. A Special report of the institute's panel on the health effects of traffic-related air pollution, Special report 17, Health Effects Institute.
- Hopke, P.K., Cohen, D.D., Begum, B.A., Biswas, S.K., Ni, B., Pandit, G.G., Santoso, M., Chung, Y.S., Davy, P., Markwitz, A., Waheed, S., Siddique, N., Santos, F.L.,

- Pabroa, P.C.B., Seneviratne, M.C.S., Wimolwattanapun, W., Bunprapob, S., Vuong, T.B., Duy Hien, P. and Markowicz, A. (2008). Urban air quality in the Asian region. *Sci. Total Environ.* 404: 103–112.
- Hung, N., Lee, S., Hang, N., Kongpran, J., Kim Oanh, N., Shim, S. and Bae, G. (2014). Characterization of black carbon at roadside sites and along vehicle roadways in the Bangkok Metropolitan Region. *Atmos. Environ.* 92: 231–239.
- Hyvärinen, A.P., Vakkari, V., Laakso, L., Hooda, R.K., Sharma, V.P., Panwar, T.S., Beukes, J.P., van Zyl, P.G., Josipovic, M., Garland, R.M., Andreae, M.O., Pöschl, U. and Petzold, A. (2013). Correction for a measurement artifact of the Multi-Angle Absorption Photometer (MAAP) at high black carbon mass concentration levels. *Atmos. Meas. Tech.* 6: 81–90.
- Janssen, N.A., Hoek, G., Simic-Lawson, M., Fischer, P., van Bree, L., ten Brink, H., Keuken, M., Atkinson, R.W., Anderson, H.R., Brunekreef, B. and Cassee, F.R. (2011). Black carbon as an additional indicator of the adverse health effects of airborne particles compared with PM₁₀ and PM_{2.5}. *Environ. Health Perspect.* 119: 1691–1699.
- Ježek, I., Ktrašnik, T., Westerdahl, D. and Močnik, G. (2015). Black carbon, particle number concentration and nitrogen oxide emission factors of random in-use vehicles measured with the on-road chasing method. *Atmos. Chem. Phys.* 15: 11011–11026.
- JICA (Japan International Cooperation Agency) (2014). Roadmap for transport infrastructure development for metro Manila and ITS surrounding areas (Region III & Region IV-A). Technical Report No. 2, Transport Demand Analysis. ALMEC Corporation. <http://www.neda.gov.ph/wp-content/uploads/2015/03/FR-TR2-TECHNICAL-ANALYSIS.-12149639.pdf>.
- Karjalainen, P., Pirjola, L., Heikkilä, J., Lähde, T., Tzamkiozis, T., Ntziachristos, L., Keskinen, J. and Rönkkö, T. (2014). Exhaust particles of modern gasoline vehicles: A laboratory and an on-road study. *Atmos. Environ.* 97: 262–270.
- Kecorius, S., Madueño L., Vallar E., Alas, H., Betito, G., Birmili, W., Cambaliza M.O., Catipay, G., Galvez, M.C., Lorenzo, G., Müller, T., Simpas, J.B., Tamayo, E.G. and Wiedensohler, A. (2017). Aerosol particle mixing state, soot number size distributions, and emission factors in a polluted urban environment: Case study of Metro Manila, Philippines. *Atmos. Environ.* 170: 169–183.
- Kim Oanh, N., Upadhyay, N., Zhuang, Y., Hao, Z., Murthy, D., Lestari, P., Villarin, J., Chengchua, K., Co, H. and Dung, N. (2006). Particulate air pollution in six Asian cities: Spatial and temporal distributions, and associated sources. *Atmos. Environ.* 40: 3367–3380.
- Kim, K., Woo, D., Lee, S. and Bae, G. (2015). On-road measurements of ultrafine particles and associated air pollutants in a densely populated area of Seoul, Korea. *Aerosol Air Qual. Res.* 15: 142–153.
- Kompalli, S.K., Babu, S.S., Moorthy, K.K., Manoj, M., Kumar, N.K., Shaeb, K.H. and Joshi, A.K. (2014). Aerosol black carbon characteristics over Central India: Temporal variation and its dependence on mixed layer height. *Atmos. Res.* 147–148: 27–37.
- Krzyzanowski, M., Kuna-Dibbert, B. and Schneider, J. (2005). *Health effects of transport-related air pollution*. WHO Regional Office Europe.
- Krzyzanowski, M. and Cohen, A. (2008). Update of WHO air quality guidelines. *Air Qual. Atmos. Health* 1: 7–13.
- Krzyzanowski, M. (2012). *Health effects of black carbon*. World Health Organization, Copenhagen.
- Latha, K.M. and Badarinath, K. (2005). Seasonal variations of black carbon aerosols and total aerosol mass concentrations over urban environment in India. *Atmos. Environ.* 39: 4129–4141.
- Lee, S., Bae, G., Park, S. and Jung, S. (2007). Black carbon pollution level at a roadside of Seoul in spring. *J. Korean Soc. Atmos. Environ.* 23: 466–477.
- Lena, T.S., Ochieng, V., Carter, M., Holguin-Veras, J. and Kinney, P.L. (2002). Elemental carbon and PM_{2.5} levels in an urban community heavily impacted by truck traffic. *Environ. Health Perspect.* 110: 1009–1015.
- Lenschow, P., Abraham, H.J., Kutzner, K., Lutz, M., Preuß, J.D. and Reichenbacher, W. (2001). Some ideas about the sources of PM₁₀. *Atmos. Environ.* 35: 23–33.
- Levy, I., Mihele, C., Lu, G., Narayan, J., Hilker, N. and Brook, J.R. (2014). Elucidating multipollutant exposure across a complex metropolitan area by systematic deployment of a mobile laboratory. *Atmos. Chem. Phys.* 14: 7173–7193.
- Mahalakshmi, D., Badarinath, K. and Naidu, C. (2011). Influence of boundary layer dynamics on pollutant concentrations over urban region - A study using ground based measurements. *Indian J. Radio Space Phys.* 40: 147–152.
- Nemmar, A., Hoet, P.H.M., Vanquickenborne, B., Dinsdale, D., Thomeer, M., Hoylaerts, M.F., Vanbilloen, H., Mortelmans, L. and Nemery, B. (2002). Passage of inhaled particles into the blood circulation in humans. *Circulation* 105: 411–414.
- Nerrière, É., Zmirou-Navier, D., Blanchard, O., Momas, I., Ladner, J., Le Moullec, Y., Personnaz, M.B., Lameloise, P., Delmas, V., Target, A. and Desqueyroux, H. (2005). Can we use fixed ambient air monitors to estimate population long-term exposure to air pollutants? The case of spatial variability in the Genotox ER study. *Environ. Res.* 97: 32–42.
- Patton, A.P., Laumbach, R., Ohman-Strickland, P., Black, K., Alimokhtari, S., Liou, P.J. and Kipen, H.M. (2016). Scripted drives: A robust protocol for generating exposures to traffic-related air pollution. *Atmos. Environ.* 143: 290–299.
- Peters, J., Theunis, J., Van Poppel, M. and Berghmans, P. (2013). Monitoring PM₁₀ and ultrafine particles in urban environments using mobile measurements. *Aerosol Air Qual. Res.* 13: 509–522.
- Peters, J., Van den Bossche, J., Reggente, M., Van Poppel, M., De Baets, B. and Theunis, J. (2014). Cyclist exposure to UFP and BC on urban routes in Antwerp, Belgium. *Atmos. Environ.* 92: 31–43.
- Petzold, A. and Schönlinner, M. (2004). Multi-angle

- absorption photometry – A new method for the measurement of aerosol light absorption and atmospheric black carbon. *J. Aerosol Sci.* 35: 421–441.
- Petzold, A., Ogren, J., Fiebig, M., Laj, P., Li, S., Baltensperger, U. and Zhang, X. (2013). Recommendations for reporting "black carbon" measurements. *Atmos. Chem. Phys.* 13: 8365–8379.
- Philippine Land Transportation Office Annual Report 2015, <http://www.lto.gov.ph/transparency-seal/annual-reports/file/19-annual-report-2015.html>, Last Access: 27 March 2017.
- Philippine Population Density (Based on the 2015 Census of Population), <http://psa.gov.ph/content/philippine-population-density-based-2015-census-population>, Last Access: 20 September 2016.
- Philippines, Department of Environment and Natural Resources, Environmental Management Bureau (2012). *National Air Quality Status Report 2010-2011*. Quezon City: DENR.
- Rakowska, A., Wong, K.C., Townsend, T., Chan, K.L., Westerdahl, D., Ng, S., Močnik, G., Drinovec, L. and Ning, Z. (2014). Impact of traffic volume and composition on the air quality and pedestrian exposure in urban street canyon. *Atmos. Environ.* 98: 260–270.
- Ruths, M., Bismarck-Osten, C.V. and Weber, S. (2014). Measuring and modelling the local-scale spatio-temporal variation of urban particle number size distributions and black carbon. *Atmos. Environ.* 96: 37–49.
- Schneider, J., Kirchner, U., Borrmann, S., Vogt, R. and Scheer, V. (2008). In situ measurements of particle number concentration, chemically resolved size distributions and black carbon content of traffic-related emissions on German motorways, rural roads and in city traffic. *Atmos. Environ.* 42: 4257–4268.
- Song, S., Wu, Y., Xu, J., Ohara, T., Hasegawa, S., Li, J., Yang, L. and Hao, J. (2013). Black carbon at a roadside site in Beijing: Temporal variations and relationships with carbon monoxide and particle number size distribution. *Atmos. Environ.* 77: 213–221.
- Tripathi, S.N., Dey, S. and Tare, V. (2005). Aerosol black carbon radiative forcing at an industrial city in northern India. *Geophys. Res. Lett.* 32: L08802.
- Tuch, T.M., Haudek, A., Müller, T., Nowak, A., Wex, H., and Wiedensohler, A. (2009). Design and performance of an automatic regenerating adsorption aerosol dryer for continuous operation at monitoring sites. *Atmos. Meas. Tech.* 2: 417–422.
- Van den Bossche, J., Peters, J., Verwaeren, J., Botteldooren, D., Theunis, J. and Baets, B.D. (2015). Mobile monitoring for mapping spatial variation in urban air quality: Development and validation of a methodology based on an extensive dataset. *Atmos. Environ.* 105: 148–161.
- Van den Bossche, J., Theunis, J., Elen, B., Peters, J., Botteldooren, D. and Baets, B.D. (2016). Opportunistic mobile air pollution monitoring: A case study with city wardens in Antwerp. *Atmos. Environ.* 141: 408–421.
- Van Poppel, M., Peters, J. and Bleux, N. (2013). Methodology for setup and data processing of mobile air quality measurements to assess the spatial variability of concentrations in urban environments. *Environ. Pollut.* 183: 224–233.
- Westerdahl, D., Fruin, S., Sax, T., Fine, P.M. and Sioutas, C. (2005). Mobile platform measurements of ultrafine particles and associated pollutant concentrations on freeways and residential streets in Los Angeles. *Atmos. Environ.* 39: 3597–3610.
- Westerdahl, D., Fruin, S., Fine, P. and Sioutas, C. (2008). The Los Angeles International Airport as a source of ultrafine particles and other pollutants to nearby communities. *Atmos. Environ.* 42: 3143–3155.
- WHO (2016, May 12). Air pollution levels rising in many of the world's poorest cities. <http://www.who.int/media/centre/news/releases/2016/air-pollution-rising/en/>, Last Access: 22 April 2017.
- WHO (2016, September 27). WHO releases country estimates on air pollution exposure and health impact. <http://www.who.int/mediacentre/news/releases/2016/air-pollution-estimates/en/>, Last Access: 22 April 2017.
- WHO Regional Office for Europe, & World Health Organization (2006). *Air quality guidelines: Global update 2005: Particulate matter, ozone, nitrogen dioxide, and sulfur dioxide*. World Health Organization, Geneva.
- Wiedensohler, A., Birmili, W., Nowak, A., Sonntag, A., Weinhold, K., Merkel, M., Wehner, B., Tuch, T., Pfeifer, S., Fiebig, M., Fjåraa, A.M., Asmi, E., Sellegri, K., Depuy, R., Venzac, H., Villani, P., Laj, P., Aalto, P., Ogren, J.A., Swietlicki, E., Williams, P., Roldin, P., Quincey, P., Hüglin, C., Fierz-Schmidhauser, R., Gysel, M., Weingartner, E., Riccobono, F., Santos, S., Gröning, C., Faloon, K., Beddows, D., Harrison, R., Monahan, C., Jennings, S.G., O'Dowd, C.D., Marinoni, A., Horn, H.G., Keck, L., Jiang, J., Scheckman, J., McMurry, P.H., Deng, Z., Zhao, C.S., Moerman, M., Henzing, B., de Leeuw, G., Löschau, G. and Bastian, S. (2012). Mobility particle size spectrometers: Harmonization of technical standards and data structure to facilitate high quality long-term observations of atmospheric particle number size distributions. *Atmos. Meas. Tech.* 5: 657–685.
- Wiedensohler, A., Birmili, W., Putaud, J. and Orgen, J. (2014). Recommendations for aerosol sampling. In *Aerosol science: Technology and applications*, Colbeck, I. and Lazaridis, M. (Eds.), John Wiley & Sons, Chichester, pp. 45–60.
- Williams, R.D. and Knibbs, L.D. (2016). Daily personal exposure to black carbon: A pilot study. *Atmos. Environ.* 132: 296–299.
- Zhu, T., Melamed, M., Parrish, D., Gauss, M., Klenner, L.G. and Lawrence, M. (2012). *WMO/IGAC impacts of megacities on air pollution and climate*. GAW Report No. 205, World Meteorological Organization, Geneva.

Received for review, August 21, 2017

Revised, December 25, 2017

Accepted, January 1, 2018